Biophysical Letter

Deactivation of a Negative Regulator: A Distinct Signal Transduction Mechanism, Pronounced in Akt Signaling

Anisur Rahman[1] and Jason M. Haugh[1,*]
[1]Department of Chemical and Biomolecular Engineering, North Carolina State University, Raleigh, North Carolina

ABSTRACT Kinase cascades, in which enzymes are sequentially activated by phosphorylation, are quintessential signaling pathways. Signal transduction is not always achieved by direct activation, however. Often, kinases activate pathways by deactivation of a negative regulator; this indirect mechanism, pervasive in Akt signaling, has yet to be systematically explored. Here, we show that the indirect mechanism has properties that are distinct from direct activation. With comparable parameters, the indirect mechanism yields a broader range of sensitivity to the input, beyond saturation of regulator phosphorylation, and kinetics that become progressively slower, not faster, with increasing input strength. These properties can be integrated in network motifs to produce desired responses, as in the case of feedforward loops.

Received for publication 22 July 2014 and in final form 1 October 2014.

*Correspondence: jason_haugh@ncsu.edu

Phosphorylation of proteins and lipids, catalyzed by specific kinase enzymes, is ubiquitous in intracellular signal transduction. A classic example in eukaryotes is the canonical structure of the mitogen-activated protein kinase cascades, in which three kinases are sequentially activated by phosphorylation (1). Another example is the PI3K (phosphoinositide 3-kinase)/Akt pathway, which (like the mammalian mitogen-activated protein kinases) is prominently dysregulated in human cancers (2). Type-I PI3Ks phosphorylate a lipid substrate to produce the lipid second messenger, PIP_3, which recruits the protein kinase Akt and mediates its activation by phosphorylation (3,4). In no small part because of these important pathways, we typically think of phosphorylation as a direct means of activating molecular interactions and reactions in signal transduction. This is not the only way to increase the flux through a signaling pathway, however. Consider signaling downstream of Akt, which phosphorylates a host of protein substrates to affect diverse functions. A survey of the Akt signaling hub shows that many of these reactions result in a decrease, rather than an increase, in activity/function of the substrates (3). And, among those substrates, the four listed in Table 1 are considered negative, not positive, regulators of downstream signaling (see Fig. S1 in the Supporting Material). Whereas negative regulators are appreciated for their roles in feedback adaptation of signaling, the implications of deactivating a negative regulator as an indirect mechanism of pathway activation has yet to be explored.

Here, we use simple kinetic models to elucidate the basic properties of pathway activation by deactivation of a negative regulator (hereafter referred to as mechanism II), as compared with the standard activation of a positive regulator (mechanism I). The analysis is presented in the context of protein phosphorylation, but the conclusions may be generalized to other reversible modifications or to allosteric binding interactions. The common first step is phosphorylation of the regulatory molecule by the kinase. The activity of the upstream kinase such as Akt may be represented by a dimensionless, time (t)-dependent input signal function, $s(t)$. We assume that the total amount of regulator is constant and define its phosphorylated fraction as $\phi(t)$. Neglecting concentration gradients and saturation of the upstream kinase and of the opposing (constitutively active) phosphatase(s), the conservation of phosphorylated regulator is expressed as follows (see Text S1 in the Supporting Material):

$$\frac{d\phi}{dt} = k_p[s(1-\phi)-\phi];\ \ \phi(0) = 0. \qquad (1)$$

The parameter k_p is the pseudo-first-order rate constant of protein dephosphorylation. In the case of s = constant (i.e., subject to a step change at $t = 0$), the properties of this simplified kinetic equation are well known (5) and may be summarized as follows. As the magnitude of the signal strength s increases, the steady-state value of ϕ, ϕ_{ss}, increases in a saturable fashion; when $s >> 1$, ϕ_{ss} approaches its maximum value of 1 and is insensitive to further increases in s. The kinetics of $\phi(t)$ approaching ϕ_{ss} become progressively faster as s increases, however.

Next, we model the influence of the regulator on a downstream response. Defining the fractional response as ρ and

Editor: H. Wiley.

http://dx.doi.org/10.1016/j.bpj.2014.10.003

TABLE 1 Survey of Akt substrates and downstream signaling

Substrate (site)	Effect on substrate	Outcome
TSC2 (T1462)	GAP activity ↓	Rheb, mTOR ↑
PRAS40 (T246)	mTOR binding ↓	mTOR ↑
GSK3α/β (S21/S9)	kinase activity ↓	β-catenin ↑
BAD (S136)	Bcl-2/xL binding ↓	Bcl-2/xL ↑

following analogous assumptions as above, we formulate equations for mechanisms I and II as follows:

$$\frac{d\rho}{dt} = \begin{cases} [k_{a,0} + (k_{a,\max} - k_{a,0})\phi](1-\rho) - k_{d,0}\rho & \text{(I)} \\ k_{a,0}(1-\rho) - [k_{d,0} - (k_{d,0} - k_{d,\min})\phi]\rho & \text{(II)}. \end{cases} \quad (2)$$

In each equation, the first term on the right-hand side describes activation, and the second, deactivation. In mechanism I, the effective rate constant of activation increases linearly with ϕ, from a minimum value of $k_{a,0}$ when $\phi = 0$ up to a maximum value of $k_{a,\max}$ when $\phi = 1$; the deactivation rate constant is fixed at $k_{d,0}$. Conversely, in mechanism II, the effective rate constant of deactivation decreases linearly with ϕ, from a maximum value of $k_{d,0}$ when $\phi = 0$ down to a minimum value of $k_{d,\min}$ when $\phi = 1$; in this mechanism, the activation rate constant is fixed at $k_{a,0}$. The initial condition is assigned so that ρ is stationary when $\phi = 0$. To further set the two mechanisms on a common basis, we define dimensionless parameters such that the maximum steady-state value of ρ (with $\phi_{ss} = 1$) is the same for both mechanisms I and II,

$$g = k_{a,\max}/k_{a,0} = k_{d,0}/k_{d,\min}; \quad K = k_{a,0}/k_{d,0}. \quad (3)$$

With these definitions, each conservation equation is reduced to the following dimensionless form:

$$\frac{1}{k_{d,0}}\frac{d\rho}{dt} = \begin{cases} K[1 + (g-1)\phi](1-\rho) - \rho & \text{(I)} \\ K(1-\rho) - [1 - (1-g^{-1})\phi]\rho & \text{(II)}. \end{cases} \quad (4)$$

Mechanisms I and II (Fig. 1 *a*) are compared first at the level of their steady-state solutions, ρ_{ss}, for stationary s. Equation 1 yields the familiar hyperbolic dependence of ϕ_{ss} on s, and $\rho_{ss}(s)$ has the same shape for both mechanisms. However, whereas ρ_{ss} of mechanism I shows saturation at a lower value of s than ϕ_{ss}, the opposite is true of mechanism II (Fig. 1 *b*). Thus, mechanism II retains sensitivity to the input even while phosphorylation of the upstream regulator shows saturation. This is perhaps more readily seen when $\phi_{ss}(s)$ is replaced with a sigmoidal Hill function (i.e., with s replaced by s^n in Eq. 1) (Fig. 1 *c*). The key parameter that affects the relative sensitivities of mechanisms I and II and the disparity between them is the gain constant, g (see Text S1 in the Supporting Material). As this parameter is increased, ρ_{ss} of mechanism I becomes increasingly saturable with respect to ϕ_{ss} (Fig. 1 *d*), whereas ρ_{ss} of mechanism II gains sensitivity as ϕ_{ss} approaches 1 (Fig. 1 *e*). As an illustrative example, consider that when ϕ_{ss} is increased from 0.90 to 0.95, or from 0.98 to 0.99, the amount of the negative regulator in the active state is reduced by a factor of 2 (see Fig. S2).

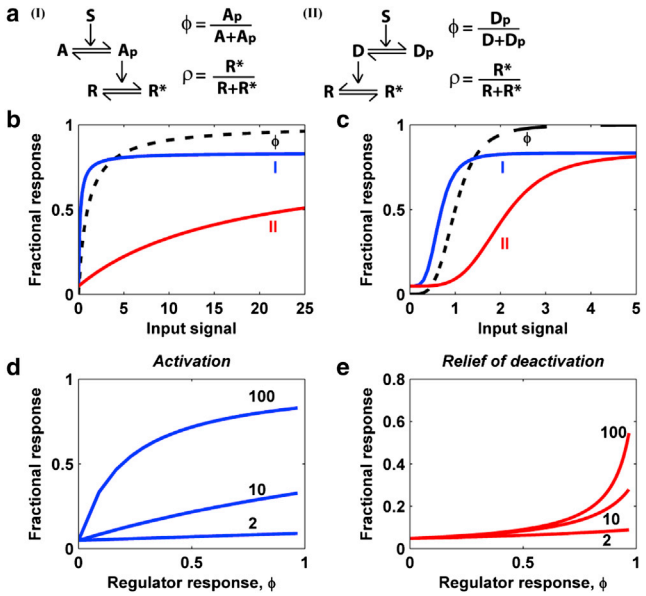

FIGURE 1 Steady-state properties of mechanisms I and II. (*a*) Schematics of direct (I) and indirect (II) activation. (*b*) Steady-state dose responses, $\rho_{ss}(s)$, of mechanisms I and II along with phosphorylation of the upstream regulator, $\phi_{ss}(s)$ (Eq. 1 at steady state); $K = 0.05$, $g = 100$. (*c*) Same as panel *b*, except with a sigmoidal $\phi_{ss}(s)$ (Hill function with $n = 4$). (*d*) Steady-state output, ρ_{ss}, of mechanism I vs. ϕ_{ss} for $K = 0.05$ and indicated values of the gain constant, g. (*e*) Same as panel *d*, but for mechanism II. To see this figure in color, go online.

The two mechanisms also show distinct temporal responses. In the response of mechanism I to a step increase in s, $\rho(t)$ approaches ρ_{ss} with a timescale that generally becomes faster as s increases. Unless the kinetics of $\phi(t)$ are rate-limiting, the timescale is ~$k_{d,0}^{-1}(1-\rho_{ss})$ (Fig. 2 *a*; see also Text S1 and Fig. S3 in the Supporting Material). Conversely, the response of mechanism II generally becomes slower as s increases, inasmuch as the frequency of deactivation decreases whereas that of activation is constant, with a timescale of ~$k_{a,0}^{-1}\rho_{ss}$ (Fig. 2 *b*). To approximate a transient input, we model $s(t)$ as a step increase followed by a decay. For mechanism I, the response $\rho(t)$ is such that the variation in the time of the peak, as a function of the step size, is modest. The subsequent decay is prolonged when $\phi(t)$ hovers close to saturation (Fig. 2 *c*). Such kinetic schemes have been analyzed in some detail previously (6,7). In contrast, the response of mechanism II to the transient input is such that the system retains sensitivity and consistent decay kinetics beyond the saturation of $\phi(t)$. The distinctive feature is that $\rho(t)$ peaks noticeably later in time as the magnitude of the peak increases (Fig. 2 *d*).

Having established the basic steady state and kinetic properties of mechanism II as compared with the canonical mechanism I, we considered what outcomes could be achieved by linking these motifs in series or in parallel. Such schemes are identified in the Akt/mTOR signaling network, for example (see Fig. S4). In a standard kinase

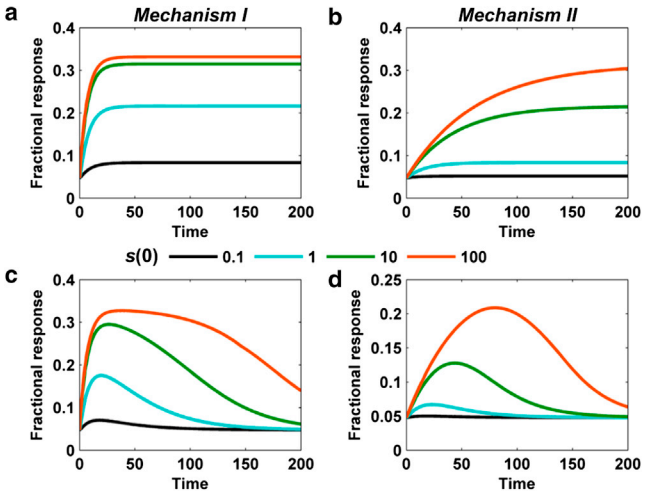

FIGURE 2 Kinetic properties of mechanisms I and II. (*a*) Response of mechanism I to a step change in *s* from zero to the indicated *s*(0). Time is given in units of $k_p t$; parameters are $K = 0.05$, $g = 10$, and $k_{d,0} = 0.1k_p$. (*b*) Same as panel *a*, but for mechanism II. (*c*) Same as panel *a*, but for a transient input, $s(t) = s(0)\exp(-0.03k_p t)$. *d*) Same as panel *c*, but for mechanism II. To see this figure in color, go online.

activation cascade, it is understood that the properties of saturation and sensitivity are compounded with each step of the cascade (8). Thus, two sequential steps of mechanism I yield progressive saturation of the steady-state output at lower *s* (Fig. 3 *a*), and the desaturating effect of mechanism II is likewise compounded (Fig. 3 *b*). By corollary it follows that a sequence of mechanisms I and II will show an intermediate dose response; that is, the mechanism II step offsets the saturation effect of mechanism I.

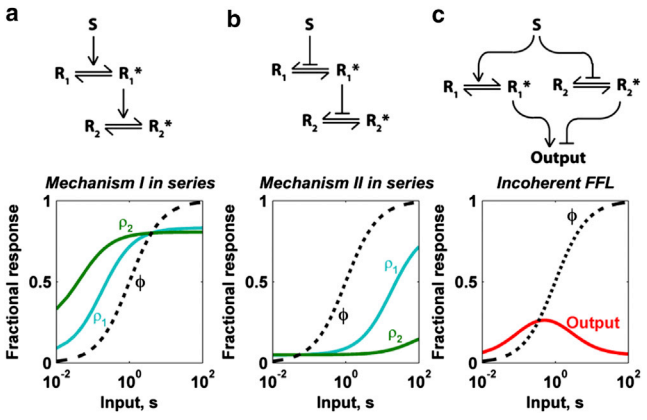

FIGURE 3 Serial and parallel schemes incorporating mechanism I or/and II. (*a*) Steady-state outputs of two response elements, ρ_1 and ρ_2, activated by mechanism I in series. At each level, $K = 0.05$, $g = 100$. (*b*) Same as panel *a*, but for mechanism II in series. (*c*) Incoherent feedforward loop (FFL) in which mechanisms I and II are activated in parallel to activate and inhibit, respectively, the terminal output. For both mechanisms I and II, $K = 0.05$, $g = 100$. The parameters for Eq. 5 are $\alpha = 2.5$, $\beta = 50$. To see this figure in color, go online.

A more complex scheme is to combine the two mechanisms in parallel, as in an incoherent feedforward loop (FFL) connected to an "AND NOT" output as follows:

$$\text{Output} = \alpha\rho_I/(1 + \alpha\rho_I + \beta\rho_{II}). \quad (5)$$

Given the differential saturation properties of mechanisms I and II, this scheme readily yields the expected biphasic dose response (9) without the need for disparate values of the parameters (Fig. 3 *c*). Regarding the kinetics, the analysis shown in Fig. 2 makes it clear that mechanism II naturally introduces time delays in cascades or network motifs. Thus, for the incoherent FFL at high, constant *s*, activation of inhibition by mechanism II would tend to yield a dynamic response marked by a peak followed by adaptation (see Fig. S5). Analogous calculations were carried out for a coherent FFL as well (see Fig. S6).

To summarize our conclusions and their implications for signaling downstream of Akt and other kinases, we have described a distinct, indirect signal transduction mechanism characterized by deactivation of a negative regulator. This motif shows steady-state sensitivity beyond saturation, and therefore the activity of the upstream kinase, such as Akt, can be relatively high. By comparison, the direct activation of signaling by phosphorylation requires that activity of the kinase be regulated, or specifically countered by high phosphatase activity, to maintain sensitivity and avoid saturation of the response. The mechanism described here also introduces relatively slow kinetics (for comparable parameter values). This property, together with its extended range of sensitivity, would allow the motif to be incorporated in signaling networks to yield desired steady and unsteady responses in a robust manner. Considering that key signaling processes mediated by Akt (notably activation of the mammalian target of rapamycin (mTOR) pathway) are achieved by deactivation of negative regulators, we assert that greater recognition of this mechanism and of its distinct properties is warranted.

SUPPORTING MATERIAL

Additional supplemental information and six figures are available at http://www.biophysj.org/biophysj/supplemental/S0006-3495(14)01053-4.

ACKNOWLEDGMENTS

This work was supported by grant No. R01-GM088987 from the National Institutes of Health, Bethesda, MD.

REFERENCES and FOOTNOTES

1. Dhillon, A. S., S. Hagan, …, W. Kolch. 2007. MAP kinase signaling pathways in cancer. *Oncogene.* 26:3279–3290.

2. Yuan, T. L., and L. C. Cantley. 2008. PI3K pathway alterations in cancer: variations on a theme. *Oncogene.* 27:5497–5510.

3. Manning, B. D., and L. C. Cantley. 2007. AKT/PKB signaling: navigating downstream. *Cell.* 129:1261–1274.

4. Fayard, E., G. D. Xue, …, B. A. Hemmings. 2010. Protein kinase B (PKB/Akt), a key mediator of the PI3K signaling pathway. *In* Phosphoinositide 3-Kinase in Health and Disease, *Vol. 1*.. Springer-Verlag, Berlin, Germany, pp. 31–56.

5. Lauffenburger, D. A., and J. L. Linderman. 1993. Receptors: Models for Binding, Trafficking, and Signaling. Oxford University Press, New York.

6. Behar, M., N. Hao, …, T. C. Elston. 2008. Dose-to-duration encoding and signaling beyond saturation in intracellular signaling networks. *PLOS Comput. Biol.* 4:e1000197.

7. Haugh, J. M. 2012. Live-cell fluorescence microscopy with molecular biosensors: what are we really measuring? *Biophys. J.* 102:2003–2011.

8. Kholodenko, B. N., J. B. Hoek, …, G. C. Brown. 1997. Quantification of information transfer via cellular signal transduction pathways. *FEBS Lett.* 414:430–434.

9. Kaplan, S., A. Bren, …, U. Alon. 2008. The incoherent feed-forward loop can generate non-monotonic input functions for genes. *Mol. Syst. Biol.* 4:203.

Text S1: Modeling Supplement

Deactivation of a negative regulator: a distinct signal transduction mechanism, pronounced in Akt signaling

Anisur Rahman and Jason M. Haugh

Development of the model

Our modeling approach here was to make simplifying assumptions so as to minimize the number of adjustable parameters and allow for ready understanding of the presented analyses. It should be appreciated that a more realistic model of a particular signaling process would integrate additional interactions and modifications, and complexities such as subcellular localization/compartmentalization might need to be included. In our view, more sophisticated modeling will be warranted once quantitative measurements corresponding to the modeled variables become available.

We consider two distinct mechanisms by which a protein kinase might promote signal transduction through substrate phosphorylation: (I) increasing the activity of a positive regulator (activator) or (II) decreasing that of a negative regulator (deactivator). In both cases, the common step is phosphorylation of the regulatory molecule by the kinase. To describe this in the simplest manner possible, we consider that the relative activity of the upstream kinase may be represented by a time-dependent rate constant, $k_k(t)$. Neglecting concentration gradients and saturation of the upstream kinase or of the opposing (constitutively active) phosphatase(s), we express the conservation of phosphorylated activator (mechanism I) as follows.

$$\frac{dA_p}{dt} = k_k(t)A - k_pA_p; \quad A_p(0) = 0 \tag{S1}$$

In the equation above, A_p is the concentration of phosphorylated activator, A is the concentration of unphosphorylated activator, and k_p is the pseudo-first-order rate constant of protein dephosphorylation. With the assumption that the sum of the phosphorylated and unphosphorylated regulator is conserved during the time scale of interest, we define the fraction of phosphorylated regulator as the dimensionless variable, ϕ, and we define the dimensionless signal function, $s(t)$, to scale $k_k(t)$ by k_p.

$$A + A_p = A_{Tot} = \text{constant}$$
$$\phi = \frac{A_p}{A_{Tot}}; \quad s(t) = \frac{k_k(t)}{k_p} \tag{S2}$$

Substituting these definitions into Eq. S1 yields Eq. 1 in the main text, reprised here.

$$\frac{d\phi}{dt} = k_p\left[s\left(1-\phi\right)-\phi\right]; \quad \phi(0) = 0$$

Up to this point, mechanism II is developed identically (i.e., Eq. 1 in the main text applies to both mechanisms), except for the conceptual distinction that the substrate of the kinase is a deactivator; therefore, D and D_p take the place of A and A_p, respectively.

Next we consider the downstream response element, which is found in either an inactive (off) or active (on) state, with concentrations R and R^*, respectively. Following analogous assumptions as above, we write conservation equations for two mechanisms — activation (mechanism I) and relief of deactivation (mechanism II) — as follows.

$$\frac{dR^*}{dt} = \begin{cases} \left(k_{a,0}A + k_{a,\max}A_p\right)A_{Tot}^{-1}R - k_{d,0}R^* & \text{(I)} \\ k_{a,0}R - \left(k_{d,0}D + k_{d,\min}D_p\right)D_{Tot}^{-1}R^* & \text{(II)} \end{cases} \tag{S3}$$

In each of these equations, the first term describes activation, and the second, deactivation. In mechanism I, the activation term contains contributions from both the unphosphorylated and phosphorylated activator, with rate constants $k_{a,0}$ and $k_{a,\max}$, respectively (dividing the activation term by the constant A_{Tot} makes these rate constants pseudo-first order); the deactivation rate constant is fixed at $k_{d,0}$. Conversely, in mechanism II, the deactivation term contains contributions from both the unphosphorylated and phosphorylated deactivator, with rate constants $k_{d,0}$ and $k_{d,\min}$, respectively (dividing the deactivation term by the constant D_{Tot} makes these rate constants pseudo-first order); in this mechanism, the activation rate constant is fixed at $k_{a,0}$. With the assumption that the total concentration of the response element ($R_{Tot} = R + R^*$) is constant, and with the definition $\rho = R^*/R_{Tot}$ (along with the definition of ϕ for each mechanism), Eq. S3 is modified to obtain Eq. 2 in the main text, reprised here.

$$\frac{d\rho}{dt} = \begin{cases} \left[k_{a,0} + \left(k_{a,\max} - k_{a,0}\right)\phi\right]\left(1-\rho\right) - k_{d,0}\rho & \text{(I)} \\ k_{a,0}\left(1-\rho\right) - \left[k_{d,0} - \left(k_{d,0} - k_{d,\min}\right)\phi\right]\rho & \text{(II)} \end{cases}$$

The initial conditions are assigned as follows, so that ρ is stationary when $\phi = 0$ for either mechanism.

$$\rho(0) = \frac{k_{a,0}}{k_{a,0} + k_{d,0}} \tag{S4}$$

To set the models for mechanisms I and II on a common basis for comparison, we enforce that both mechanisms yield the same maximum steady-state value of ρ (i.e., with $\phi_{ss} = 1$), which is achieved if we define a common, dimensionless gain parameter, g, as follows.

$$g = \frac{k_{a,\max}}{k_{a,0}} = \frac{k_{d,0}}{k_{d,\min}} \tag{S5}$$

Defining $K = k_{a,0}/k_{d,0}$, each conservation equation is reduced to a dimensionless form with only two adjustable constants (g and K) as follows. Thus, main text Eq. 2 was reduced to main text Eq. 4, reprised here.

$$\frac{1}{k_{d,0}}\frac{d\rho}{dt} = \begin{cases} K\left[1 + \left(g-1\right)\phi\right]\left(1-\rho\right) - \rho & \text{(I)} \\ K\left(1-\rho\right) - \left[1 - \left(1 - g^{-1}\right)\phi\right]\rho & \text{(II)} \end{cases}$$

$$\rho(0) = \frac{K}{1+K}$$

Analysis of the steady state

For constant s, the steady-state solution of main text Eq. 1, ϕ_{ss}, is as follows.

$$\phi_{ss} = \frac{s}{1+s} \tag{S6}$$

For each of the two mechanisms, the steady-state response ρ_{ss} is derived in terms of ϕ_{ss}, and hence in terms of s, as follows.

$$\rho_{ss} = \begin{cases} \dfrac{K\left[1+(g-1)\phi_{ss}\right]}{1+K\left[1+(g-1)\phi_{ss}\right]} = \dfrac{K(1+gs)}{1+K+(1+gK)s} & \text{(I)} \\ \dfrac{K}{1-\left(1-g^{-1}\right)\phi_{ss}+K} = \dfrac{K(1+s)}{1+K+g^{-1}(1+gK)s} & \text{(II)} \end{cases} \tag{S7}$$

To lend additional insight, the steady-state response may be expressed as a fold change relative to the basal value.

$$\frac{\rho_{ss}(s)-\rho(0)}{\rho(0)} = \begin{cases} \dfrac{(g-1)s}{1+K+(1+gK)s} & \text{(I)} \\ \dfrac{(g-1)s}{g(1+K)+(1+gK)s} & \text{(II)} \end{cases} \tag{S8}$$

As one might expect, each of these fold-change expressions can be rearranged to give the familiar hyperbolic form. Adopting the vernacular of a pharmacological dose-response relationship, we define the EC_{50} here as the value of s that yields the half-maximal value of the fold change. By rearrangement of Eq. S8, we obtain

$$EC_{50} = \begin{cases} \dfrac{1+K}{1+gK} & \text{(I)} \\ g\dfrac{1+K}{1+gK} & \text{(II)} \end{cases} \tag{S9}$$

By inspection of Eq. S9, one concludes the following.

1) The EC_{50} value of mechanism I is less than 1, the value of s for which $\phi_{ss} = 0.5$, provided that $g > 1$ (phosphorylation activates the regulator). Therefore, mechanism I generally saturates at a lower value of s relative to phosphorylation of the positive regulator. The substrate of the activator (the response element in the 'off' state) is progressively depleted as the input increases, and so there is sub-linear sensitivity of the response with respect to the increasing activity of the activator. This is the nature of a sequential activation pathway with potential for saturation at each step.
2) The EC_{50} value of mechanism II is greater than 1, the value of s for which $\phi_{ss} = 0.5$, provided that $g > 1$ (phosphorylation deactivates the regulator). Therefore, II generally saturates at a higher value of s relative to phosphorylation of the negative regulator. In this case, the

substrate of the deactivator (the response element in the 'on' state) becomes more abundant as the input increases, and so there is supra-linear sensitivity of the response with respect to the decreasing activity of the deactivator. This offsets the decreasing sensitivity of ϕ with respect to s.

3) Mechanism II has an EC_{50} value that is greater, by a factor of g, than that of I. Thus, as g is increased to enhance the maximum fold-change of the response, the dynamic range of s (over which the response shows near-linear sensitivity) shrinks for I, whereas it is expanded for II.

Since g is defined so that the maximum and minimum values of $\rho_{ss}(s)$ are the same for both mechanisms, the higher EC_{50} for mechanism II implies a lower sensitivity in the limit s, $\phi_{ss} << 1$, as shown in Fig. 1d&e. For mechanism II, greater sensitivity near saturation implies low sensitivity when the system is far from saturation, whereas the opposite is well appreciated to be true for the 'canonical' mechanism I.

Analysis of time scales

Transient behaviors of the two mechanisms are shown in Fig. 2 of the paper. The results were obtained by numerical integration of the differential equations, using a stiff implicit solver in MATLAB. Though this is simple enough, we find that approximations of the 'exact' solutions are instructive. Such analyses are outlined below.

In the examples shown in Fig. 2a&b, a step change in the input function $s(t)$ is assumed, i.e., constant s for $t > 0$. The transient solution of main text Eq. 1 for these conditions is as follows, with ϕ_{ss} taken from Eq. S6.

$$\phi(t) = \phi_{ss}\left\{1 - \exp\left[-\left(1+s\right)k_p t\right]\right\} \qquad \text{(S10)}$$

Therefore, the kinetics of $\phi(t)$ approaching the steady-state value become progressively faster as s increases, with a time scale of $[(1 + s)k_p]^{-1}$. Based on the parameter values chosen for the calculations shown in Fig. 2, we reasoned that the kinetics of $\phi(t)$ were relatively fast. With this conjecture, we substitute the approximation $\phi(t) \approx \phi_{ss}$ in main text Eq. 2 and simplify as follows.

$$\frac{d\rho}{dt} \approx \begin{cases} \dfrac{k_{d,0}}{1-\rho_{ss}}\left(\rho_{ss} - \rho\right) & \text{(I)} \\ \dfrac{k_{a,0}}{\rho_{ss}}\left(\rho_{ss} - \rho\right) & \text{(II)} \end{cases} \qquad \text{(S11)}$$

For the calculated examples, $k_{d,0} = 0.1k_p$, $k_{a,0} = 0.005k_p$, and ρ_{ss} varies from 0.047 ($s = 0$) and 0.33 ($s >> 1$). Therefore, we confirm that the time scale of $\phi(t)$ is never rate limiting under the conditions tested.

This analysis also shows how the kinetics of $\rho(t)$ for mechanism I generally become faster, and how the kinetics for II become slower, as s increases. By inspection of Eq. S11 above, we identify the characteristic time scale τ as the inverse of the effective rate constant, i.e., with $d\rho/dt \approx \tau^{-1}(\rho_{ss} - \rho)$. The time constant thusly identified for mechanism I is $(1 - \rho_{ss})/k_{d,0}$, which decreases (faster kinetics) as ρ_{ss} increases. As explained in the main text, this is intuitive because

signaling increases the frequency of activation. The time constant for mechanism II is $\rho_{ss}/k_{a,0}$, which increases (slower kinetics) as ρ_{ss} increases; here, signaling decreases the frequency of deactivation, while that of activation is constant.

In the examples shown in Fig. 2c&d, a time-decaying input was considered.

$$s(t) = s(0)\exp\left(-k_{decay}t\right) \tag{S12}$$

The rate constant of decay was $k_{decay} = 0.03k_p$, i.e., slow enough for $\phi(t)$ to respond according to the following quasi-steady state approximation.

$$\phi(t) \approx \frac{s(t)}{1+s(t)} \tag{S13}$$

It is readily shown that this function decays, on a relative basis, slower than does $s(t)$. This is intuitive when $s(t) >> 1$, because $\phi(t)$ is pegged close to 1. This insight along with the steady-state sensitivity results presented in Fig. 1d&e provides at least a qualitative explanation of the kinetics shown in Fig. 2 c&d. For mechanism I, the slow decay of $\phi(t)$ for saturating $s(0)$ is compounded by the modest sensitivity of ρ to $\phi(t)$ near saturation (Fig. 1d); thus, the response peaks rapidly but decays slowly under such conditions (Fig. 2c). In contrast, mechanism II shows ultrasensitivity to $\phi(t)$ in that regime (Fig. 1e); thus, after a prolonged equilibration period (reflected in the time at which the response achieves its peak, consistent with the slow kinetics shown in Fig. 2b), the time scale associated with the decay of the response is much closer to that of $s(t)$ (Fig. 2d).

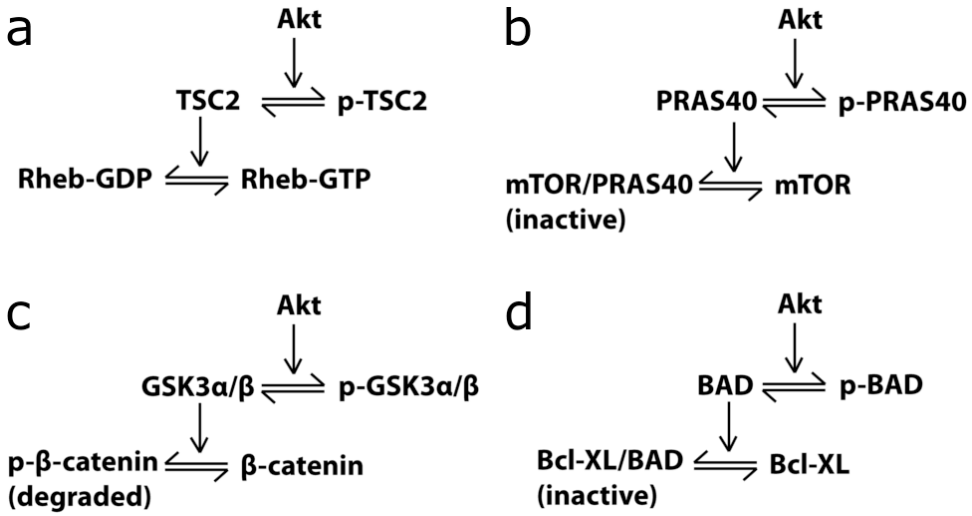

Figure S1 **Multiple examples of the indirect activation mechanism (mechanism II) downstream of Akt. In each example, the kinase activity of Akt is considered the input, and its substrate is a negative regulator (deactivator). *a*) Phosphorylation of TSC2 results in reduced GTP-activating protein (GAP) function, indirectly promoting accumulation of the active, GTP-bound form of Rheb. Rheb-GTP goes on to activate mTOR (not pictured here). *b*) Phosphorylation of PRAS40 results in 14-3-3 protein binding that prevents association with PRAS40 with mTOR. This liberates mTOR for interactions with its substrates. *c*) Phosphorylation of GSK3α/β inactivates the kinase, resulting in reduced phosphorylation of β-catenin. As a consequence, active β-catenin accumulates. *d*) Phosphorylation of BAD prevents it from binding Bcl-2/-xL. This frees Bcl-2/-xL to promote cell survival by maintaining the integrity of the outer mitochondrial membranes.**

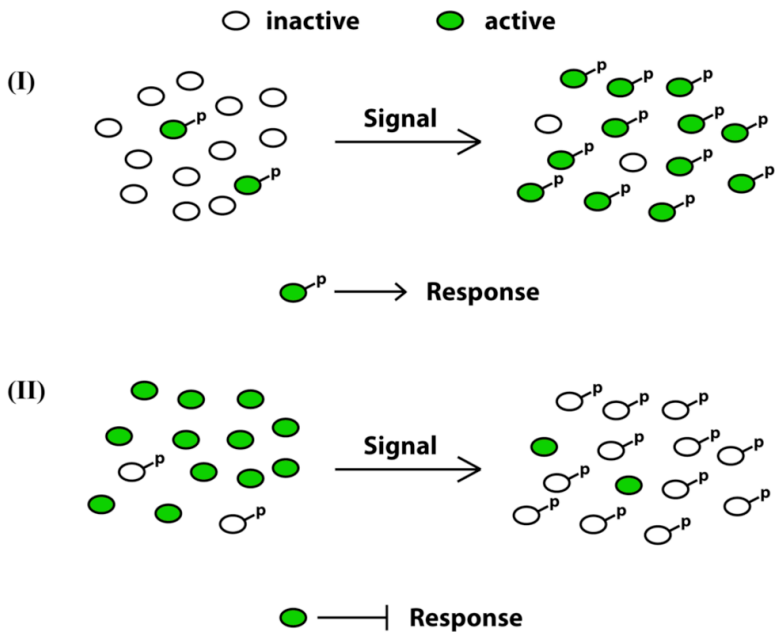

Figure S2 **Illustration of the steady-state sensitivities of mechanisms I and II as phosphorylation of the regulator approaches saturation. In both cases, progressive increases in the input signal eventually result in phosphorylation of most of the regulator (indicated by –P) at steady state. In the case of mechanism I, the regulator has a positive influence on the downstream response, and the phosphorylated form is more active. Near saturation, a further increase in the input results in only a slight fractional gain in the activity of the positive regulator. Conversely, in the case of mechanism II, the regulator has a negative influence on the downstream response, and the phosphorylated form is less active. Near saturation, a further increase in the input results in a dramatic fractional change (reduction) in the remaining activity of the negative regulator.**

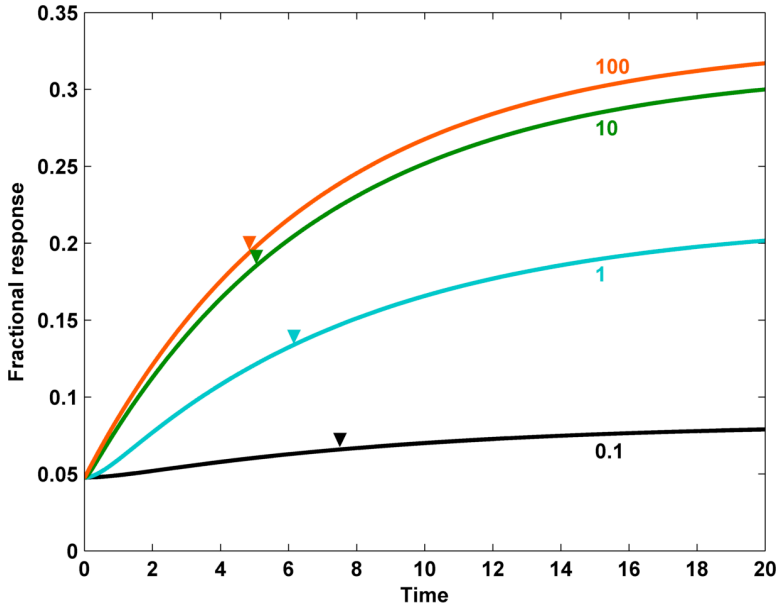

Figure S3 Replotting of Fig. 2a to better show the early kinetics. Initial responses of the direct activation mechanism (mechanism I) to step changes in s, from zero to the indicated values of $s(0)$, are shown. Time is given in units of $k_p t$; parameters are $K = 0.05$, $g = 10$, $k_{d,0} = 0.1k_p$. For each curve, the midpoint between $\rho(0)$ and ρ_{ss} is indicated by the inverted triangle, illustrating that the time scale becomes faster as the input increases.

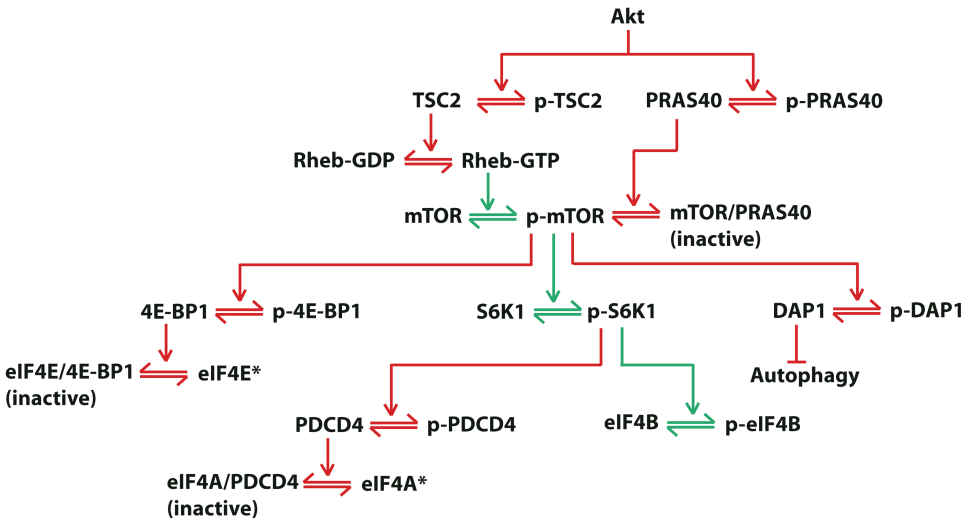

Figure S4 Identification of activation mechanisms I (green) and II (red) in the Akt/mTOR signaling network.

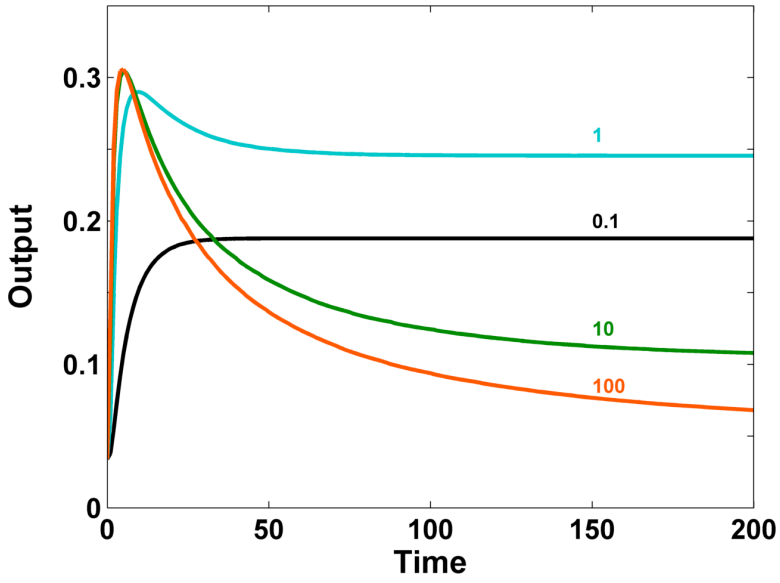

Figure S5 Temporal response of an incoherent feedforward motif with direct activation of an activator by mechanism I and indirect activation of an inhibitor by mechanism II. Parameter values are the same as in Fig. 3c, and $k_{d,0} = 0.1k_p$ for both I and II. Values of the input, s, are as indicated for each curve, and time is expressed in units of $k_p t$. Note that high values of s yield an adaptive response due to the inherent disparity in time scales for I and II.

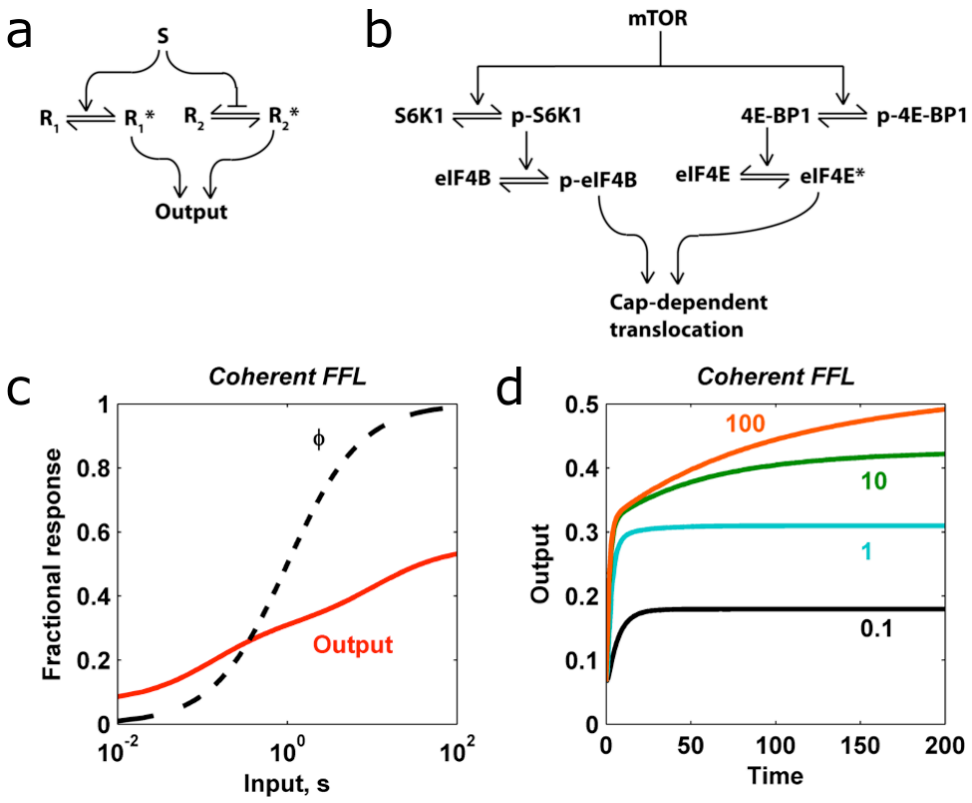

Figure S6 Analysis of a coherent feedforward loop (FFL) with direct and indirect activation of two activators in parallel. *a*) Hypothetical circuit diagram. *b*) Signaling in the mTOR network that loosely maps to the hypothetical circuit. *c*) Steady-state response of the coherent FFL, assuming additive contributions to the output, according to

$$\text{Output} = (\alpha\rho_I + \beta\rho_{II})/(1 + \alpha\rho_I + \beta\rho_{II}).$$

Parameter values are $K = 0.05$ and $g = 100$ for both I and II; the parameters for the output function are $\alpha = 0.5$, $\beta = 1$. Note that the output shows a broad sensitivity, over several logs of *s*, due to the disparity between the saturation of I and II. *d*) Kinetics of the system, with the same parameter values as in *c* and $k_{d,0} = 0.1k_p$ for both I and II. Values of the input, *s*, are as indicated for each curve, and time is expressed in units of $k_p t$. Note that high values of *s* provoke an initial rapid increase due to activation of I, followed by slower increase due to delayed activation of II.